

Mathematical Images of Planet Earth

Gabriele Gramelsberger

INTRODUCTION

Since the 1970s we have grown used to the outside view of planet Earth, mediated either by satellite images or simulation images of computer models of the planet's atmosphere and climate. These views from the outside evoke the impression that we see an object, the planet Earth, and that everything we see in these images is representative of real states of the planet. However, this is not the case for most of today's images of Earth. What we really see are images of mathematical narrations of Earth. The reasons for this are the following: today's imaging of Earth always involves enormous amounts of mathematics, either for satellite views like NASA's Blue Marble: Next Generation or for visualized model versions based on the computer simulation known as General Circulation Atmosphere and Ocean Models (AOGCMs).¹ Although satellite images count as empirical data while model visualizations apply as virtual data, both data types share the same mathematical narration of Earth. This mathematical narration is given by physico-mathematical theory, in particular by hydro- and thermodynamics, and is employed in algorithms that drive satellite devices as well as simulation models. Interestingly, advanced measurement technologies like satellite-based Light Detection and Ranging (LIDAR) involve three to four times more software code – and, in turn, mathematics – than atmosphere and ocean models.² Thus, the core question of this paper is: How much mathematics do we

¹ | Cf. National Aeronautics and Space Administration (NASA) 2014.

² | See section 5 of this paper.

see in Earth images? Or to put it differently: What does mathematics contribute to our global views of our world?

Understanding today's imaging techniques of Earth is not easy since mathematics, algorithms, and advanced technologies are employed. Thus, this paper aims at a deeper understanding of the increasingly complex constitution of satellite images as well as simulation images of computer models of planet Earth. It will briefly discuss what is seen when Earth is observed from the outside (orbital view). It continues with an outline of the physical and mathematical narration of Earth as a processable entity (physico-mathematical view), followed by a discussion of the shift in measurement devices from photo cameras to spectrometers (decoded view), and the constraints of an algorithmic handling (algorithmic view). Finally, the merging of all these views constructing images of Earth as algorithmic objects will be discussed (merged process view).

THE ORBITAL VIEW OF PLANET EARTH



Fig. 1: *Blue Marble* (National Aeronautics and Space Administration (NASA), 1972)³

The original *Blue Marble* – an image of the earth taken by the crew of the Apollo 17 spacecraft in December 1972 from a distance of 45,000 km – shows a cloud-surrounded sphere embedded in the blackness of space (fig. 1). The photograph was shot with a 70-mm photo camera

3 | Cf. Poole 2008.

and an 80-mm lens. It presents a huge cyclone roaming over the Indian Ocean (white), the land masses of Antarctica (white) and Africa (green-brown), and parts of the Indian and Atlantic Oceans (blue).⁴ As 80% of the atmosphere's mass and 99% of its water vapor (clouds) is located in the troposphere (0 to 12 km), the visible sphere has a real diameter of 12,742 km plus 12 km. From this circumstance two implications follow. First, this view of Earth shows one of the main visible weather phenomena, namely cloud cover, indicating the atmosphere's circulation. Usually more than 60% of Earth is covered by clouds – ranging in horizontal size from 30 m to 4,000 km and persisting between 10 minutes and 10 days. Thus, a completely cloud-free view of the entire planet is usually not given and imaging Earth means primarily imaging clouds. Second, depending on the camera and the lens, the orbital view of the whole globe requires a minimum distance of about the geostationary orbit an altitude of 35,786 km.⁵ Thus, the International Space Station (ISS) orbits at an altitude of 416 km, and most of the earth observation satellites cover only parts of Earth's surface. For instance, low earth orbit (LEO) satellites usually operating at an altitude of 800 km cover swaths of several hundred to a few thousand kilometers of Earth's surface.⁶ Therefore data from various satellites are used to compose a global view.

4 | Due to the convention that the North Pole is at the top of maps the photograph has been rotated.

5 | Geosynchronous orbit satellites (GEO) are located in a circular orbit 35,786 km above the earth's equator following the direction of the earth's rotation. Thus, their position remains the same for an observer on Earth. Cf. European Space Agency (ESA) 2014.

6 | Low earth orbit (LEO) satellites, in general, operate from 160 km (orbital period of about 88 minutes) to 2,000 km altitude (orbital period of about 127 minutes), but most earth observation LEO satellites are located in about 800 km altitude. Cf. *Ibid.*

	Classification	Altitude	Phenomena/Devices
Moon	Lunar distance to Earth	363,104 to 405,696 km	
Space	Space	>10,000 km	GOS satellites (35,786 km); Van Allen Belt (15,000 to 25,000 km)
Atmosphere	Exosphere	700 to 10,000 km	LEO earth observation satellites (800 km)
	Thermosphere (Ionosphere)	80 to 700 km	ISS (416 km); Aurora borealis
	Mesosphere	50 to 80 km	Noctilucent clouds
	Stratosphere	12 to 50 km	Nacreous clouds; weather balloons; ozone layer
	Troposphere	0 to 12 km	Weather; airplanes
Earth	Earth diameter (Equator)	12,742 km	

Tab. 1: Locating the orbital view (information gathered from NASA and ESA websites)

Nevertheless, the global view of planet Earth was developed long before mankind built air- and spacecraft to explore the sky and atmosphere. This Earth-based global view is composed from a perspective that covers a horizontal length scale on the order of 1,000 to 2,500 km. The so-called synoptic perspective has been developed since the mid-19th century, when meteorological data were gathered systematically by standardized observations from weather stations on the ground, mainly using thermometers (temperature), barometers (air pressure), hygrometers (humidity), and anemometers (wind speed) – data that were internationally communicated via telegraph. This early synoptic view is a purely empirical perspective, which has derived from the shift of local observations into regionally and internationally coordinated data. The appropriate data-gathering tools used to compile this view were synoptic weather maps connecting singular data with isolines, e.g. isobars for equal values of air pressure.⁷ Thus, the status of air masses became visible on the

7 | Cf. Schneider/Nocke (ed.) 2014; Gramelsberger 2017.

maps as isobars indicate weather patterns like cyclones – low air pressure systems causing movement in the atmosphere (wind and storms) and precipitation (rain, hail, snow). From very early on, isobar maps like the map of December 1887 (fig. 2) began displaying changes in air pressure systems, thus making visible the dynamics of air masses roaming over large areas. This led to the development of a theory of cyclogenesis often indicated by clouds, but also the desire to forecast the near future of the dynamic behavior of the atmosphere's circulation.⁸

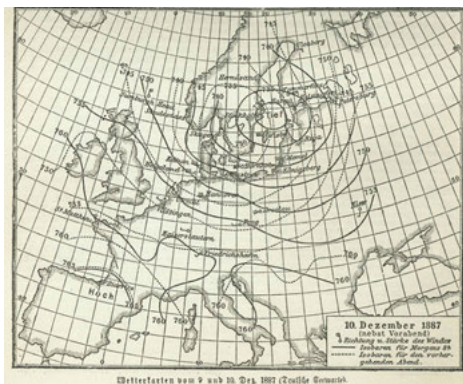


Fig. 2: *Synoptic view: isobar map of 9th and 10th December 1887 with high air pressure systems (»hoch«) and low air pressure systems (»tief«) (Deutsche Seewarte, 1887)*

THE PHYSICO-MATHEMATICAL VIEW OF PLANET EARTH

When 60% of Earth is covered by clouds, clouds can be seen as visible indicators of atmospheric processes, in particular of the global circulation of the atmosphere. Lacking an outside global view before the invention of satellites, such a global view on atmospheric circulation could only be conceptually developed by scientists. Such a view is conceived

8 | For instance, Robert Fitzroy, a British Admiral to the Navy, became very early interested in forecasting storms. He developed a theory of air movement, forces, and duration of motion, which he called 'dynametry'. His intent was to extract wind forecasts from local measurement data by combining statistical and mathematical methods. Cf. Fitzroy 1863.

physically by taking into account the differences in solar radiation for low and high latitudes⁹, the earth's rotation¹⁰, the differences in the speed of rotation at each point on the planet¹¹, and the Coriolis effect.¹² All these physical causes add up to global circulation patterns that are responsible for regional weather phenomena by moving huge masses of cold and warm, dry and humid air around the globe. In other words, warm air in the tropics expands, becomes lighter, rises, drains off to the side in higher regions of the atmosphere (air pressure falls), and causes a vertical flow, which drives global circulation. Conversely, cold air sinks and becomes heavier (air pressure rises). Differences in temperature result in differences in air pressure, which, in turn, lead to mechanical work, that is, motion based on the air's expansion and contraction. Thus, the atmosphere is scientifically conceived as a giant air mass circulation and heat engine driven by solar radiation and gravitational forces. These forces are expressed in terms of local differences of seven measurable variables: wind velocity (in three directions), air density, air pressure, temperature, and humidity.

The interactions of these seven variables are expressed by hydro- and thermodynamic theory. Hydrodynamic theory goes back to Isaac Newton's second law of motion ($F = m \cdot a$)¹³, which was expanded to explain fluids by Leonhard Euler and George G. Stokes.¹⁴ Thermodynamic theory is rooted in Ludwig Boltzmann's statistical theory of heat.¹⁵ The advantage of such a physical theory is that it can be expressed mathematically. Hydrodynamics includes Euler's equation of motion and thus allows for the description of the development of a fluid gaseous system like Earth's atmosphere. Using hydro- and thermodynamic theory turned meteorology into the physics of the atmosphere, not only able to describe the current state of the atmosphere but to forecast future developments – as aptly outlined by Vilhelm Bjercknes in 1904:

9 | Cf. Halley 1686.

10 | Cf. Hadley 1735.

11 | Cf. Dove 1837.

12 | Cf. Ferrel 1858.

13 | The alteration of motion or force (F), respectively, is equal to the mass (m) of an object multiplied by the acceleration (a) of the object. Cf. Newton 1687.

14 | Cf. Euler 1954; Stokes 1980.

15 | Cf. Boltzmann 1896/98.

The necessary and sufficient conditions for a rational solution of the problem of meteorological prediction are the following: 1. One has to know with sufficient accuracy the state of the atmosphere at a certain time [measurements]. 2. One has to know with sufficient accuracy the laws [hydro- and thermodynamics] according to which a certain state of the atmosphere develops from another.¹⁶

Consequently, Bjerknes developed a first mathematical model of global circulation based on the three hydrodynamic equations of motion (describing the relation between the three velocity components, density and air pressure), the continuity equation (expressing the continuity of mass during motion), the equation of state for the atmosphere (articulating the relation between density, air pressure, temperature and humidity of any air mass), and the two fundamental theorems in the mechanical theory of heat (specifying how the energy and entropy of any air mass change in a change of state). This mathematical model of the air mass circulation and heat engine makes the seven observables (wind velocity in three directions, air density, air pressure, temperature, humidity) computable and thus projectable into future. It constitutes the core of every weather and climate model even today. Furthermore, it offers two additional advantages: First,

while measurements cannot comprise all state variables of the climate system in their full spatio-temporal extension, climate models can represent each state variable at any desired time or location within the model domain. [Second,] like cyberspace, one can navigate through the model data to experience a physically consistent virtual world. While experiments with the climate system are not feasible, climate models are the virtual laboratory of geoscientists.¹⁷

THE DECODED VIEW OF PLANET EARTH

Questions on this physico-mathematical view of Earth's atmosphere have to be expressed in terms of process-indicating state variables, e.g. differences in temperature, air pressure, etc. The answers are delivered empirically by direct measurements using thermometers, barometers, hygrom-

16 | Bjerknes 2009, 663; Cf. Gramelsberger 2009.

17 | Feichter 2011, 216.

eters, etc., which then are presented in tables of figures, simple graphs, or isolines. However, direct measurement methods have been increasingly complemented with indirect methods of remote sensing, ever since Sputnik collected data for the *International Geophysical Year* from 1957 to 1958. As satellite-based measurements cannot probe the atmosphere directly, remote sensing is indispensable to transform empirical data into theory- and assumption-laden data. Why? First, satellite data require a shift to spectrometer devices that record electromagnetic signals remotely. Second, the information contained in electromagnetic signals has to be decoded by mathematical methods. Third, satellite data have become accessible via Graphical User Interfaces (GUIs) and thus manipulatable.

A typical modern signal decoding device is the Infrared Sounder (IRS) of the European Meteosat Third Generation. It is based on an imaging Fourier-interferometer for obtaining information on the atmosphere's temperature and humidity.¹⁸ Fourier interferometry means that raw data are computed from interference in the observed electromagnetic signals.¹⁹ The differences of the amplitudes of the interfering signals contain the information that has to be decoded mathematically by Fourier transform. Based on this mathematical method of signal decoding, increasing information can be read off the raw data. Thus, in recent years more than 50 different Essential Climate Variables (ECV) have become observable with these increasingly sophisticated measurement devices, delivering new answers to new questions about climate change.²⁰

Another important signal decoding technology, which is increasingly changing environmental observation, is LIDAR (light detection and ranging) for both air- and space-borne use.²¹ LIDAR actively meas-

18 | Cf. World Meteorological Organization (WMO) 2014a.

19 | Cf. Johnston 2001.

20 | Cf. World Meteorological Organization (WMO) 2010.

21 | »Three decades ago, with the incoming of the laser, the world has witnessed its particular evolution and application to the study of the atmosphere. In fact, the atmosphere was one of the first sites where the properties of the laser light (high power, monochromaticity, short pulse duration and collimation), were put on trial. With the invention of ruby lasers, generators of powerful optical pulses in the year of 1962, the use of the laser in remote optical probing was made possible.« (Castrejón-García et al. 2002, 513).

ures differences in wavelengths by sending out short pulses of laser light in the order of nanoseconds and then decoding information about the composite of the atmosphere from these differences. Thus it is possible to monitor the distribution of tiny particles of industrial emissions such as soot, dust, and aerosols—fine solid particles or liquid droplets. The basic assumption is that laser pulses interact with particles and are backscattered with a time delay. The backscattered laser light (number of received photons = intensity) is captured in the LIDAR device by an optical telescope, background radiation is filtered out, and the remaining optical signal is converted by photodiodes into an electrical signal and amplified. Finally the amplified electrical signal is converted by digitizers into a digital signal.

Typically, lidar systems require a sampling rate on the order of 100 million samples (MS)/s, which leads to a spatial resolution on the order of $1/2 \times (300 \text{ m}/\mu\text{s})/(100 \text{ MS/s}) = 1.5 \text{ m}$. [...] The required capture time of 100 μs at a sampling rate of 100 MS/s gives a waveform size of 10,000 points. Modern PC-based digitizers with ultrafast PCI transfer speeds are able to capture 10,000-point waveforms at rates in excess of 1000 waveforms per second.²²

However, because the number of signals is too large, 1,000 to 10,000 single samples are averaged as one measurement and stored as raw data for further algorithm-based data evaluations and visualizations.²³ Nevertheless, LIDAR does not measure single particles, but records an echo of the particle distribution of the atmosphere.

Depending on the size of the particles, the backscattered laser beams undergo changes in wavelength (elastic/inelastic backscattering), which show characteristic signatures: small particles cause Rayleigh scattering (atoms, molecules) while bigger particles cause Mie scattering (aerosol particles).²⁴ In the age of anthropogenic climate change the vertical distribution of the extinction coefficient of aerosols is of particular interest, because it allows scientists to infer the influence of aerosols on the radiation of sunlight (cooling or warming effect). However, the inference of the particle types, their size, and distribution from the characteristic

22 | Dawson 2005.

23 | Cf. Cornelisen 2005, 5.

24 | Cf. Strutt 1899-1920; Mie 1908.

signature is embedded in the mathematical equation and has to be decoded by deriving a solution for the characteristic signature equation. Unfortunately, the solution of the signature equation – a (Bernoulli type) ordinary differential equation – yields incorrect results. In the words of James D. Klett, one of the leading LIDAR researchers of the 1980s, the signature equation »has a tendency to produce at best marginal results, and in practice has likely been more a source of frustration than a useful tool for analyzing radar or lidar returns. [...] Worse yet, others have noted the solution may lead to »... absurdly large, infinite, or negative values ...« and »... physically meaningless ...« results.²⁵ Remember that the only information LIDAR provides are numerical values. Thus, it is not easy to evaluate what is physically meaningless and what is meaningful. However, in 1981 Klett found a practical solution for the derivation of the characteristic signature by changing the limits of the integral. Since then the so-called Klett method has been used in most LIDAR systems, but it has the disadvantage that the LIDAR ratio (extinction to backscatter ratio) must be estimated based on assumptions. »The Klett retrieval method requires a reference point, where the atmospheric backscatter value is known. This reference point calibrates the rest of the points in the measurement.²⁶ Thus, LIDAR technologies have to be complemented with in-situ measurements or, for satellites, with more complex spectrometric measurements.

THE ALGORITHMIC VIEW OF PLANET EARTH

Inversely decoded information from electromagnetic signals, which count as »empirical« data, as well as mathematical models for simulation, which count as »virtual« data, are not only purely mathematical ways of obtaining data – they are solely accessible by computation. Thus, the LIDAR equation as well as the hydro- and thermodynamic model of the atmosphere have to be provided algorithmically. The algorithmic view translates the mathematical general view – describing the interactions between the variables and parameters – into an extensive set of instructions that can be worked through step by step by a computer. What can

²⁵ | Klett 1981, 212. Cf. Klett 1985.

²⁶ | Marchant 2008, 57.

be written down in a short equation has to be transformed into a narratable `if, then/else-plot` embedded in `>do/end do<`-loops. An enormous amount of additional knowledge is necessary to create such narratable instructions to make a computer do work like measuring or simulating. Every constant, every variable, every operation has to be specified with exact numbers or instructions, respectively. No ambiguity is allowed, otherwise the program would crash. Interestingly, LIDAR algorithms involve many more lines of code than simulation models for the atmosphere and the ocean. While the LIDAR-equation as well as the hydro- and thermodynamic model of the atmosphere can be written down in one line of mathematical symbols, the algorithms require many more code lines. In raw numbers, the ADM-Aeolus LIDAR measurement products are based on 340,000 code lines, while the ECHAM5 atmosphere model consists of 65,700 code lines.²⁷

Furthermore, the general mathematical approach has to be discretized for stepwise calculation. This means that the time has to be fragmented into time steps and space into layers of grid points. This is true both for measurement and for simulation methods. For instance, the »new space-borne lidar and radar [technology] will record profiles continuously every 0.1 s, so for the data to be processed in a satisfactory time, an accurate lidar forward model is required that runs in less than 0.001 s.«²⁸ For simulating an atmosphere model the globe is discretized into a grid of computing points, which represent an average distance of 500 to 110 km at the equator and up to 60 horizontal layers (fig. 3). Depending on the spatial resolution, an atmosphere model is computed within 10- to 20-min time steps for a time period ranging from a minimum of 30 years up to several hundreds of years.²⁹

27 | The Atmospheric Dynamics Mission (ADM-Aeolus) is an ESA satellite of the Earth Explorer Mission series carrying a LIDAR system for sounding air currents. ECHAM5 was one of the 22 atmosphere models of the fourth IPCC report. Cf. Reitebuch 2011; ECHAM5 2008.

28 | Hogan 2006, 5984.

29 | Climate is defined by the World Meteorological Organization (WMO) as the average weather for minimum 30 years.

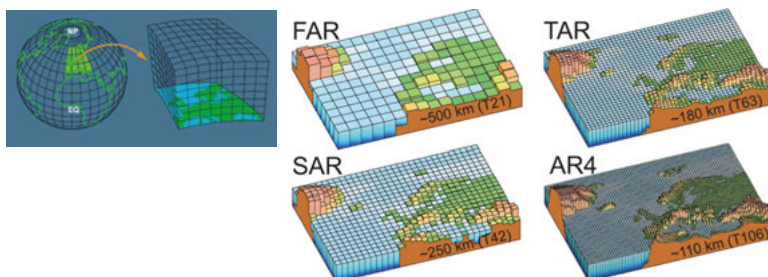


Fig. 3: (left) Digital atmosphere of a climate model (DKRZ, 2005); (middle, right) resolution of scenario calculations for the first (FAR) to the fourth (AR4) IPCC Assessment Reports (left: German Climate Computing Centre (DKRZ) 2005; right: Solomon et al. 2007, 113).

Thus, measurements as well as simulations deliver a discretized view of planet Earth. Whether or not phenomena become visible depends on the pixel size. For instance, an atmosphere model computed for a resolution of 500 km provides a very coarse view, in which small countries are represented by a handful of values for the main variables like temperature, humidity, pressure, etc. It is obvious that such a coarse view does not reveal much. In particular, it does not represent clouds, storms, or other local weather phenomena. Therefore, it is the aim of climate modelers to run their models with increasing resolution down to cloud-resolving size of approximately 2 km. However, increasing resolution requires enormous computing resources. For a cloud-resolving two-kilometer grid, computation of a global atmosphere model would have to increase by an order of 106, which is far beyond today's computer capacities.³⁰ For current satellite devices like the Flexible Combined Imager (FCI) of the European Meteosat Third Generation imagery standard, a 2-km spatial resolution is achieved for the solar spectral domain (0.4 μm to 2.1 μm) and a 1-km spatial resolution for the thermal spectrum (3.8 μm to 13.3 μm).³¹

This discretized view comes along with another problem, as most of the measurement and simulation grids differ from each other and data have to be assimilated. Projects like the Global Data Assimila-

30 | Cf. Randall et al. 2003.

31 | Cf. European Organisation for the Exploitation of Meteorological Satellite (EUMESAT) 2014.

tion System (GDAS) of the National Climatic Data Center in the U.S. merge heterogeneous observation data from various sources—surface observations, balloon data, wind profiler data, aircraft reports, buoy observations, radar observations, and satellite observations – into a homogeneous gridded space.³² Therefore, mathematical techniques like interpolation methods, filtering techniques, and other statistical strategies are employed.³³ Data assimilation »merges the observations into the [simulated] model data by optimizing the fit between real observations and data predicted by the model« and thus creating »data models« with the backing of »model data«.³⁴

CONCLUSION: THE MERGED VIEW OF PLANET EARTH

It is obvious that differences between inversely decoded observations and simulation results are vanishing. Data models (indirect observational data) merge in-situ with in-silico model data (simulation models) of planet Earth due to underlying physical and mathematical principles that are the same for both views. Measurement as well as simulation data increasingly become »data products« based on elaborate visualization algorithms. And these data products are even more heavily interpreted data. For instance NASA's *Blue Marble: Next Generation* image series (2012) shows images spatially composed from data of various satellites and temporally composed by averaging months of measurements (fig. 4). As the aim was to present a »cloud-free« image series, clouds had to be differentiated from ice and supplementary information about the landmasses beneath the clouds had to be added. In NASA's own words:

From a computer processing standpoint, the major improvement is the development of a new technique for allowing the computer to automatically recognize and remove cloud-contaminated or otherwise bad data – a process that was previously done manually. [...] However,] in tropical lowlands, cloud cover during the rainy

32 | Cf. NOAA National Climatic Data Center (NCDC) 2014.

33 | Cf. Edwards 2010; Lahoz/Khattatov/Menard (ed.) 2010.

34 | Feichter 2011, 214.

season can be so extensive that obtaining a cloud-free view of every pixel of the area for a given month may not be possible.³⁵



Fig. 4: *Blue Marble: Next Generation* (NASA, 2012)³⁶

Another example is Moderate Resolution Imaging Spectroradiometers (MODIS) data, which were used to compose the cloud-free *Blue Marble: Next Generation* images, but also other ›purified‹ data products.³⁷ »The

35 | National Aeronautics and Space Administration (NASA) 2012. Furthermore, »deep oceans are not included in the source data; the creator of the Blue Marble uses a uniform blue color for deep ocean regions, and this value has not been completely blended with observations of shallow water in coastal areas. The lack of blending may, in some cases, make the transition between shallow coastal water and deep ocean appear unnatural.« (NASA 2012. Cf. Stöckli et al. 2005).

36 | NASA Earth Observatory 2012.

37 | The Moderate Resolution Imaging Spectroradiometers (MODIS) acquiring atmospheric, oceanic, and terrestrial data in 36 spectral bands cover a range of the electromagnetic spectrum from 0.4 to 14.4 µm. MODIS was developed by NASA starting in the 1980s and was launched in space in 1999 and 2002 on board NASA's Terra and Aqua satellites. Although only two MODIS instruments have been built and launched into space, the success is shown in more than »6,500 scientific papers [...] using MODIS data.« (Tucker/Yager 2011, 14. Cf. Salomonson et al. 1989).

atmospheric correction algorithm removes water vapor and aerosols in order to achieve the intrinsic measurement of land surface spectral reflectance as if there were no atmosphere, taking into account atmospheric absorption and scattering, surface bidirectional effects, and surface adjacency effects.³⁸ The same holds for LIDAR data, which are used not only for environmental, but also for military and agricultural purposes. For instance, »contours derived directly from lidar data are accurate but not ›clean‹ and often require a level of interpolation, simplification, smoothing, or manual editing to achieve the intuitive product most people are used to.«³⁹ New visualization methods like »lidargrammetry« use »the intensity values from the lidar points as the ›photo‹ that is processed, using point elevations, into a three-dimensional image.«⁴⁰

Visualization and correction algorithms increasingly present measurement data as 2D and 3D images, concealing the enormous mathematical and theoretical efforts in order to create images from heterogeneous, discretized data.⁴¹ But these 2D and 3D images, although displaying a photographic aesthetic, are by no means photographs. The 1972 Blue Marble image can be called a photograph, but the 2012 Blue Marble: Next Generation image series definitively not. While the Apollo 17 astronauts used a Hasselblad camera, today's satellite-based imagery are multi-purpose spectrometer devices for sensing the entire electromagnetic spectrum – from visible light (VIS) to near-infrared (NIR), short-wave infrared (SWIR), mid-wave infrared (MWIR), and the long-wave infrared (LWIR) range.⁴² However, without mathematics the electromagnetic signals do not reveal anything.

Of course, standards have been established to ensure significant evidence that these images represent »empirical« data.⁴³ But these standards are stretchy and the boundaries to fictional images are fluid. As these merged views exhibit a photographic aesthetics, their fictionality is difficult to sense. What is missing is a theory to approach, describe,

38 | Tucker/Yager 2011, 11.

39 | Schmid et al. 2008, 19.

40 | Ibid.

41 | Cf. Aspey et al. 2008.

42 | Cf. World Meteorological Organization (WMO) 2014b.

43 | Cf. NDEP Guidelines 2004; ASPRS Guidelines 2004; FGDC Guidelines 1998.

and explain these types of photograph-like images. Following Frieder Nake's concept of the surface (visibility) and subface (computability) of computer based images – both mediated by the interface (human-machine interactability) – these images have to be understood as »algorithmic signs« or »algorithmic objects«, respectively.

The screen is the surface, the display buffer is the subface of the algorithmic object [..., which] comes as a visible appearance for us. At the same time, it comes as a computable appearance to the program. [...] It does not make any sense to talk about the computer image without keeping in mind its visibility and computability, i.e. its computable visibility and its visible computability.⁴⁴

Furthermore, as Nake explains, »what is usually called the interface between human and machine appears as the coupling of surface and subface. Both are machine-bound. Both are faces at which one process ends, and another process starts.«⁴⁵

Simulation images of computer models as well as satellite images are algorithmic objects, merging visibility with computability and interactability. In particular interactability turns satellite data into manipulatable objects. Instead of printed tables of figures, graphs, and isolines, Graphical User Interfaces (GUIs) make manipulations to achieve more readable, more instructive, and more accessible data products. The cloud-free Blue Marble: Next Generation images perfectly represent this amendable approach to scientific measurement by removing

44 | Nake 2008, 105. Kathrin Friedrich has introduced Frieder Nake's concept of »algorithmic signs« for scientific images in the context of computational medicine and biology. »Nake's technical semiotics stresses the fact that computational structures and processes always need to have an aesthetic surface to be amenable by humans. What appears on the computer screen is at the same time computer signal and visible sign. The visible surface is an »ambiguous figure« in that it can be explored by looking at its superficial aesthetics as well as at its »subface« (the algorithmic codes), while both determine each other.« (Friedrich 2013, 219).

45 | Nake 2008, 107. »The human places rather trivial components onto the surface (like mouse positions, or menu selections). [...] Once the surface is transformed into the subface, the program starts its signal processes, which consist of chains of determinations like any other process on a machine.« (ibid.).

›bad data.‹⁴⁶ The plasticity of the mathematical and computational basis makes these images almost arbitrarily interpretable, because, »the program is really behaving just like any other machine: it is carrying out exactly [...] what our parameter settings force it to do.«⁴⁷ But when the parameter settings tell what should be there, a new type of ›distortion‹ is added to these ›purified‹ images – a purpose-intended ›distortion‹ for imaging reasons, in addition to the common mathematical techniques of extra- and interpolating, composing, averaging, discretizing, and generalizing. This contradicts our expectations of real images when we see these ›photorealistic‹ views of planet Earth. Neither does a cloud-free Earth exist nor are most of the satellite images taken from such a distance that they capture the whole planet. Instead, the outside view of our planet Earth is an illusion created by advanced imagery.

BIBLIOGRAPHY

Aspey, Robin A. et al.: »LABVIEW graphical user interface for precision multichannel alignment of Raman lidar at Jet Propulsion Laboratory, Table Mountain Facility«, in: *Review of Scientific Instruments* 79 (2008), article 094502, doi: 10.1063/1.2976672.

ASPRS Guidelines: Vertical Accuracy Reporting for Lidar Data, American Society for Photogrammetry and Remote Sensing (ASPRS), 2004, <http://www.asprs.org>.

Boltzmann, Ludwig E.: *Vorlesungen über Gastheorie*, vol. 2, Leipzig: Barth 1896/98.

Bjerknes, Vilhelm: »Das Problem der Wettervorhersage, betrachtet von Standpunkt der Mechanik und Physik«, in: *Meteorologische Zeitschrift* 21 (1904), 1-7, translated into English and reprinted in: *Meteorologische Zeitschrift* 18 (2009), 663-667.

Castrejón-García, Rafael et al.: »The laser-backscattering equations and their application to the study of the atmospheric structure«, in: *Revista Mexicana de Física* 48:6 (2002), 513-518.

Cornelsen, Scott S.: Electronics Design of the AGLITE-LIDAR Instrument. Master Thesis in Electrical Engineering, Utah State University 2005.

46 | Cf. Stöckli et al. 2005.

47 | Nake 2008, 105.

Dawson, Andrew: »PC-based digitizers empower modern optical spectroscopy«, in: *Laser Focus World* 41:3 (2005), <http://www.laserfocusworld.com/articles/print/volume-41/issue-3> vom 27.2.2017.

Deutsche Seewarte (1875-1945), today: German Federal Service of Maritime Navigation and Hydrography: Isobar map of 9th and 10th December 1887 with high air pressure systems and low air pressure systems, Hamburg: Bundesamt für Seeschiffahrt und Hydrographie 1887.

Dove, Heinrich: *Meteorologische Untersuchungen*, Berlin: Sander 1837.

ECHAM5: File Metric Report, Hamburg: Max Planck Institute for Meteorology 2008.

Edwards, Paul: *A Vast Machine. Computer Models, Climate Data, and the Politics of Global Warming*, Cambridge: MIT Press 2010.

Euler, Leonhard: »Principes généraux du mouvement des fluids« [1755], in: Euler, Leonhard: *Opera omnia, II. Opera mathematica*, vol. 12, Zurich/Lausanne: Orell Füssli 1954, 54-91.

European Space Agency (ESA): *Earth Online* (2014), July 18th 2014, <http://earth.esa.int/>.

European Organisation for the Exploitation of Meteorological Satellite (EUMESAT): *Meteosat Third Generation (MTG)* (2014), July 26th 2014, <http://www.eumetsat.int/>.

Feichter, Johann: »Shaping Reality with Algorithms: The Earth System«, in: Gramelsberger, Gabriele (ed.): *From Science to Computational Sciences. Studies in the History of Computing and its Influence on Today's Sciences*, Zurich/Berlin: diaphanes 2011, 209-218.

Ferrel, William: »The influence of the Earth's rotation upon the relative motion of bodies near its surface«, in: *Astronomical Journal* 109 (1858), 97-100.

FGDC Guidelines: *National Standard for Spatial Data Accuracy*, The Federal Geographic Data Committee (FGDC), 1998, <http://www.fgdc.gov>.

Fitzroy, Robert: *The Weather Book: A Manual Of Practical Meteorology*, London: Longman & Green 1863.

Friedrich, Kathrin: »Digital Faces of Synthetic Biology«, in: *Studies in History and Philosophy of Biological and Biomedical Sciences* 44:2 (2013), 217-224.

Gramelsberger, Gabriele: »Conceiving meteorology as the exact science of the atmosphere – Vilhelm Bjerknes revolutionary paper of 1904«, in: *Meteorologische Zeitschrift* 18:6 (2009), 669-673.

Gramelsberger, Gabriele: »Calculating the weather – Emerging cultures of prediction in late 19th- and early 20th-century Europe«, in: Matthias Heymann, Gabriele Gramelsberger, Martin Mahony (eds.): *Cultures of Prediction in Atmospheric and Climate Science. Epistemic and Cultural Shifts in Computer-based Modelling and Simulation.*, (Routledge Environmental Humanities series), London: Routledge 2017, 45-67.

German Climate Computing Centre (DKRZ): Homepage (2005), October 20th 2005, <http://www.dkrz.de>.

Hadley, George: »The cause of the general Trade-Wind«, in: *Philosophical Transactions of the Royal Society London* 29 (1735), 58-62.

Halley, Edmund: »An historical account of the Trade-Winds and Monsoons observable in the seas between and near the Tropick, with an attempt to assign the physical cause of said Winds«, in: *Philosophical Transactions of the Royal Society London* 16 (1686), 153-168.

Hogan Robin J.: »Fast, approximate calculation of multiply scattered lidar returns«, in: *Applied Optics* 45 (2006), 5984-5992.

Johnston, Sean F.: »In search of space: Fourier spectroscopy, 1950-1970«, in: Bernward Joerges/Terry Shinn (ed.): *Instrumentation Between Science, State and Industry*, Dordrecht: Kluver Academic Publishers 2001, 121-141.

Klett, James D.: »Stable analytical inversion solution for processing lidar returns«, in: *Applied Optics* 20 (1981), 211-220.

Klett, James D.: »Lidar inversion with variable backscatter/extinction ratios«, in: *Applied Optics* 24 (1985), 1638-1643.

Lahoz, William/Khattatov, Boris/Menard, Richard (ed.): *Data Assimilation: Making Sense of Observations*, Berlin: Springer 2010.

Marchant, Christian C.: *Algorithm Development of the AGLITE-LIDAR Instrument*. Master Thesis in Electrical Engineering, Utah State University 2008.

Mie, Gustav: »Beiträge zur Optik trüber Medien, speziell kolloidaler Metalllösungen«, in: *Annalen der Physik* 25 (1908), 377-445.

Nake, Frieder: »Surface, interface, subface: Three cases of interaction and one concept«, in: Uwe Seifert/Jin H. Kim/Anthony Moore (ed.): *Paradoxes of interactivity: Perspectives for media theory, human-computer interaction, and artistic investigations*, Bielefeld: transcript 2008, 92-109.

National Aeronautics and Space Administration (NASA): Apollo Imagery (photograph AS17-148-22727) (1972), July 20th 2014, <http://spaceflight.nasa.gov/gallery/images/apollo/apollo17/html/as17-148-22727.html>.

National Aeronautics and Space Administration (NASA): Blue Marble: Next Generation (2012), July 20th 2014, <http://earthobservatory.nasa.gov/Features/BlueMarble/>.

National Aeronautics and Space Administration (NASA): Visible Earth. The Blue Marble (2014), July 18th 2014, <http://visibleearth.nasa.gov/view.php?id=57730>.

NASA Earth Observatory: The Blue Marble Next Generation (2012), October 15th 2014, <http://earthobservatory.nasa.gov/Features/BlueMarble/>.

Newton, Isaac: *Philosophiae Naturalis Principia Mathematica*, London: Royal Society 1687.

NDEP Guidelines: US-Guidelines for Digital Elevation Data, National Digital Elevation Program (NDEP) 2004, <http://www.ndep.gov>.

NOAA National Climatic Data Center (NCDC): Global Data Assimilation System (GDAS) (2014), October 20th 2014, <http://www.emc.ncep.noaa.gov/gmb/gdas/>.

Poole, Robert: *Earthrise: How man first saw the Earth*, New Haven: Yale University Press 2008.

Randall, David A. et al.: »Breaking the cloud parameterization deadlock«, in: *Bulletin of the American Meteorological Society* 84 (2003), 1547-1564.

Reitebuch, Oliver: »Lidar measurements. No observation without algorithms« (presentation charts, October 14th 2011), Munich-Oberpfaffenhofen: DLR Institute for Physics of the Atmosphere 2011.

Salomonson, Vincent V. et al.: »MODIS – Advanced Facility Instrument for Studies of the Earth as a System«, in: *IEEE Transactions on Geoscience and Remote Sensing* 27:2 (1989), 145-153.

Schmid, Keil et al.: *Lidar 101: An Introduction to Lidar Technology, Data, and Applications*, National Oceanic and Atmospheric Administration (NOAA): Costal Service Center 2008.

Schneider, Birgit/Nocke, Thomas (ed.): *Image Politics of Climate Change. Visualizations, Imaginations, Documentations*, Bielefeld: transcript (etc.) 2014.

Solomon, Susan et al.: Climate Change 2007: The Physical Science Basis, Cambridge: Cambridge University Press 2007.

Stöckli, Reto et al.: »The Blue Marble Next Generation – A true color Earth dataset including seasonal dynamics from MODIS«, in: NASA Earth Observatory (2005), <http://earthobservatory.nasa.gov/Features/BlueMarble/bmng.pdf>

Stokes, George G.: »On the theories of the internal friction of fluids in motion« [1845], in: George G. Stokes: Mathematical and Physical Papers, vol. 1. Cambridge: Cambridge University Press, 1980, 75-115.

Strutt, John William (Lord Rayleigh): »On the Scattering of Light by small Particles«, in: John William Strutt: Scientific papers, vol. 1 (1869-1881), Cambridge: Cambridge University Press 1899-1920, 104-111.

Tucker, Compton J./Yager, Karina A.: »Ten Years of MODIS in space: lessons learned and future perspectives«, in: Italian Journal of Remote Sensing, 43:3 (2011) 7-18.

World Meteorological Organization (WMO): GCOS Essential Climate Variables (2010), July 17th 2014, http://www.wmo.int/pages/prog/gcos/index.php?name=Essential_ClimateVariables.

World Meteorological Organization (WMO): Observing Systems Capability Analysis and Review Tool (OSCAR): List of all Instruments (2014a), July 18th 2014, <http://www.wmo-sat.info/oscar/instruments>.

World Meteorological Organization (WMO): Global Observing System (GOS) (2014b), July 18th 2014, <http://www.wmo.int/pages/prog/www/OSY/GOS.html>.

